PCCP

Physical Chemistry Chemical Physics

rsc.li/pccp

ROYAL SOCIETY
OF **CHEMISTRY**

PAPER
Yu Wang and Kazuyuki Takeda
Double nutation cross-polarization between heteronuclear
spins in solids

Double nutation cross-polarization between heteronuclear spins in solids†

Yu Wang and Kazuyuki Takeda ⓘ *

We study transfer of magnetization from one nuclear spin species to another in solid-state nuclear magnetic resonance by cross-polarization (CP) employing radiofrequency irradiation that causes simultaneous nutations around a pair of orthogonal axes. Under such DOuble NUTation (DONUT), polarization transfer proceeds in an unexplored arena of what we refer to as the nutation frame, which represents the interaction frame with respect to the Hamiltonian that drives nutation. The effect of DONUT is to develop either the zero-quantum or double-quantum secular component of the heteronuclear dipolar interaction, causing flip-flop or flop-flop exchange of the spin states. We demonstrate DONUT CP in polycrystalline adamantane, glycine, and histidine, also examining folding of the CP spectrum under magic-angle spinning as well as the buildup behavior of the magnetization in comparison with the conventional CP scheme. In addition, we put forth a concept of spin relaxation in the nutation frame, which is a straightforward extension of the well-known concept of spin relaxation in the rotating frame.

1. Introduction

Cross-polarization (CP) is a technique of solid-state nuclear magnetic resonance (NMR) spectroscopy to enhance the sensitivity[1–3] by transferring the magnetization from one nuclear spin species, I, to another, S, through simultaneous applications of radio-frequency (rf) irradiation in such a way that the Hartmann–Hahn condition is fulfilled.[4] Usually, CP takes place in a doubly rotating frame, where the coordinate systems for I and S are rotated separately around the static magnetic field at their respective Larmor frequencies. A few exceptions include cases in which the source spins are paramagnetic electrons, where the large difference in the gyromagnetic ratios makes it rather straightforward to implement CP in the rotating frame for the source electron spins and the laboratory frame for the target nuclear spins.[5–8]

In this work, we report on CP proceeding in a different arena realized through simultaneous nutations of the source spins I around two separate magnetic fields $\mathbf{B}_1$ and $\mathbf{B}_2$ at frequencies $\omega_{1I} = -\gamma_I B_1$ and $\omega_{2I} = -\gamma_I B_2$, where γ_I is the gyromagnetic ratio of spin I. Such DOuble NUTation (DONUT) is driven by a propagator $U_I(t)$ of the form $U_I(t) = \exp(-i\omega_{1I}t\mathbf{B}_1\cdot\mathbf{I}) \exp(-i\omega_{2I}t\mathbf{B}_2\cdot\mathbf{I})$. The idea of multiple nutation was first put forth by Khaneja and Nielsen, who studied homonuclear

Division of Chemistry, Graduate School of Science, Kyoto University, 606-8502 Kyoto, Japan. E-mail: takezo@kuchem.kyoto-u.ac.jp

dipolar recoupling with the Triple Oscillating Field techniqUe (TOFU[12]), and then extended by Straasø *et al.* to the Four-Oscillating FielD (FOLD) technique.[13] Later on, DONUT was applied to heteronuclear decoupling by Takeda *et al.*[14]

Here, we restrict ourselves to DONUT with $\mathbf{B}_1 = (-\omega_{1I}/\gamma_I,0,0)$ and $\mathbf{B}_2 = (0,0,-\omega_{2I}/\gamma_I)$, so that the propagator $U_I(t)$ is represented in the form

$$U_I(t) = \exp(-i\omega_{1I}tI_x) \exp(-i\omega_{2I}tI_z). \tag{1}$$

The rf Hamiltonian $H_{\text{rf}}^I(t)$ that results in the propagator $U_I(t)$ in eqn (1) is straightforwardly obtained with $H_{\text{rf}}^I(t) = i\dot{U}_I U_I^{-1}$[14,15]:

$$H_{\text{rf}}^I(t) = H_1 + H_2(t), \tag{2}$$

$$H_1 = \omega_{1I}I_x, \tag{3}$$

$$H_2(t) = \omega_{2I}e^{-i\omega_{1I}tI_x}I_z e^{i\omega_{1I}tI_x}. \tag{4}$$

DONUT, as well as nutation around triple- and quadruple-oscillating fields,[12,13] requires smooth modulations of the rf pulses, which can be implemented with modern NMR spectrometers.

In DONUT CP, it is in the interaction frame with respect to $H_1 = \omega_{1I}I_x$ (eqn (3)) that the source spins I contact with the target spins S. To represent this interaction frame, we coin a term, the nutation frame. Then, the essence of DONUT CP can be stated conveniently as polarization transfer that takes place between the source spin I in the nutation frame and the target spin S in the rotating frame. Transformation from the rotating frame to the nutation frame is analogous to a well-known transformation from the laboratory frame to the rotating frame,

Fig. 1 (a) (left) A schematic drawing of a static magnetic field $\mathbf{B}_0$ and a magnetic field $\mathbf{B}_1$ rotating about $\mathbf{B}_0$ at the Larmor frequency $\omega_0 = -\gamma B_0$, where γ is the gyromagnetic ratio of the spins of interest. In a reference frame rotating around $\mathbf{B}_0$ at ω_0, $\mathbf{B}_0$ vanishes and $\mathbf{B}_1$ is stationary (right). (b) In addition to the rotating field $\mathbf{B}_1$, a time-dependent component, $\mathbf{B}_2$, is applied (left) such that, in the rotating frame, it draws a circular trajectory rotating at an angular frequency $\omega_1 = |\gamma|B_1$ (middle). Another transformation through rotation around $\mathbf{B}_1$ at ω_1 leads to a frame, which we call the nutation frame, in which $\mathbf{B}_1$ vanishes while $\mathbf{B}_2$ now becomes stationary (right). This work follows the convention in which the Larmor precession is clockwise for positive γ, and nutation is counterclockwise for both positive and negative γ.[9–11]

in which a static magnetic field vanishes, whereas a resonant rf field in the former becomes stationary in the latter, as described in Fig. 1(a). In DONUT, another time-dependent field $\mathbf{B}_2$ is applied, such that, in the rotating frame, $\mathbf{B}_2$ follows a circular trajectory around the stationary field $\mathbf{B}_1$ at the nutation frequency ω_{1I}. By performing a transformation from the rotating frame into the nutation frame, $\mathbf{B}_1$ vanishes and $\mathbf{B}_2$ becomes stationary (Fig. 1(b)).

So far, a number of variants of CP have been proposed.[16–29] They improve robustness against the mismatch of the Hartmann–Hahn condition and/or the efficiency of spin-locking. Conversely, one noteworthy feature of DONUT CP is the way that the spin interactions are manipulated in the nutation frame; they acquire time dependence with mixed frequencies $\omega_{1I} \pm \omega_{2I}$. This is analogous to a frequency mixer, an electrical device used to literally mix a pair of alternating current signals with different frequencies, say, ω_p and ω_q, into another pair of signals with frequencies $\omega_p \pm \omega_q$. The mixing leads to a different condition for polarization transfer from the conventional Hartmann–Hahn condition.

In the following, we describe the principle of DONUT CP, deriving the modified Hartmann–Hahn condition both in static and magic-angle spinning (MAS) cases. Then, we discuss the practical aspects of implementing DONUT using rf irradiation with modulation, with a note on the sign of the phase of the rf signals set in the transmitter of the NMR spectrometer and that of the rf field that develops inside the coil and is felt by the nuclear spins. We demonstrate ^{1}H–^{13}C DONUT CP in adamantane and glycine, and ^{1}H–^{15}N DONUT CP in histidine.

2. Theory

We consider a dipolar-coupled heteronuclear spin system, I and S, under DONUT CP, taking account of the dipolar interaction H^{IS}, the interaction H_{rf}^S corresponding to monotonic rf irradiation applied to the target spin S with an intensity ω_{1S} along, say, the x axis, and the interaction $H_{rf}^I = H_1 + H_2(t)$ of the source spin I with the rf field that drives DONUT. The net Hamiltonian $H_{rot}(t)$ in the rotating frame is represented as

$$H_{rot}(t) = H_1 + H_2(t) + H_{rf}^S + H^{IS}(t). \qquad (5)$$

Here, H_1 and $H_2(t)$ are given in eqn (3) and (4), and H_{rf}^S and H^{IS} are

$$H_{rf}^S = \omega_{1S}S_x, \qquad (6)$$

$$H^{IS}(t) = d_{IS}\sum_{k=-2}^{2}c_k e^{ik\omega_r t}I_z S_z, \qquad (7)$$

where d_{IS} is the dipolar coupling constant, given, with the gyromagnetic ratios γ_I and γ_S and the internuclear distance r_{IS}, by

$$d_{IS} = -\left(\frac{\mu_0}{4\pi}\right)\frac{\gamma_I\gamma_S\hbar}{r_{IS}^3}, \qquad (8)$$

and ω_r is the sample spinning frequency. Under MAS, the spinning axis is tilted by $\cos^{-1}(1/\sqrt{3})$ from the static field $\mathbf{B}_0$, so that the coefficient c_k in eqn (7) is represented as

$$c_0 = 0, \qquad (9)$$

$$c_{\pm 1} = \frac{\sqrt{2}}{2}\sin 2\beta e^{\pm i\gamma}, \qquad (10)$$

$$c_{\pm 2} = -\frac{1}{2}\sin^2\beta e^{\pm 2i\gamma}, \qquad (11)$$

where β and γ are the Euler angles of the internuclear vector with respect to the reference frame fixed in the spinning sample container.

The time evolution of the system is governed by a propagator $U(t)$, which is written as

$$U(t) = T\,\exp\left[-i\int_0^t dt'H_{rot}(t')\right] \qquad (12)$$

$$= U_1(t)U_2(t), \qquad (13)$$

with

$$U_1(t) = \exp(-i\omega_{1I}tI_x), \qquad (14)$$

$$U_2(t) = T\,\exp\left[-i\int_0^t dt'H_{nut}(t')\right], \qquad (15)$$

$$H_{nut}(t) = U_1^{-1}(t)(H_{rot}(t) - H_1)U_1(t). \qquad (16)$$

$H_{nut}(t)$ is the Hamiltonian in the nutation frame, *i.e.*, in the interaction frame with respect to H_1, given by

This journal is © the Owner Societies 2023

Phys. Chem. Chem. Phys., 2023, **25**, 13838–13845 | **13839**

$$H_{\text{nut}}(t) = \omega_{2I}I_z + \omega_{1S}S_x + H_{\text{nut}}^{\text{IS}}(t), \qquad (17)$$

with

$$H_{\text{nut}}^{\text{IS}} = d_{\text{IS}}\sum_{k=-2}^{2} c_k e^{ik\omega_r t}\left(I_z\cos\omega_{1I}t + I_y\sin\omega_{1I}t\right)S_z. \qquad (18)$$

By tilting the rotating frame for spin S such that the effective field points in the z direction, we rewrite $H_{\text{nut}}(t)$ as

$$H_{\text{nut}}(t) = \omega_{2I}I_z + \omega_{1S}S_z + H_{\text{nut}}^{\text{IS}}(t), \qquad (19)$$

$$H_{\text{nut}}^{\text{IS}}(t) = d_{\text{IS}}\sum_{k=-2}^{2} c_k e^{ik\omega_r t}\left(I_z\cos\omega_{1I}t + I_y\sin\omega_{1I}t\right)(-S_x). \qquad (20)$$

Another transformation of the dipolar interaction $H_{\text{nut}}^{\text{IS}}(t)$ to the interaction frame with respect to $\omega_{2I}I_z + \omega_{1S}S_z$ leads to

$$\tilde{H}_{\text{nut}}^{\text{IS}}(t) = \exp[i(\omega_{2I}I_z + \omega_{1S}S_z)t]H_{\text{nut}}^{\text{IS}}(t)\exp[-i(\omega_{2I}I_z + \omega_{1S}S_z)t]$$

$$= d_{\text{IS}}\sum_{k=-2}^{2} c_k e^{ik\omega_r t} \qquad (21)$$

$$\times \left(I_z\cos\omega_{1I}t + I_y\sin\omega_{1I}t\cos\omega_{2I}t + I_x\sin\omega_{1I}t\sin\omega_{2I}t\right) \qquad (22)$$

$$\times \left(-S_x\cos\omega_{1S}t + S_y\sin\omega_{1S}t\right),$$

which can be rewritten as

$$\tilde{H}_{\text{nut}}^{\text{IS}}(t) = -\frac{1}{2}d_{\text{IS}}\sum_{k=-2}^{2} c_k e^{ik\omega_r t}$$

$$\times \left[I_z\cos\omega_{1I}t + \frac{1}{4}\left(I_+e^{-i\Delta t} + I_-e^{i\Delta t}\right) - \frac{1}{4}\left(I_+e^{i\Sigma t} + I_-e^{-i\Sigma t}\right)\right]$$

$$\times \left(S_+e^{i\omega_{1S}t} + S_-e^{-i\omega_{1S}t}\right), \qquad (23)$$

where Δ and Σ are defined to be the difference and the sum of the nutation frequencies ω_{1I} and ω_{2I}:

$$\Delta = \omega_{1I} - \omega_{2I}, \qquad (24)$$

$$\Sigma = \omega_{1I} + \omega_{2I}. \qquad (25)$$

Now, the Hartmann–Hahn conditions can be obtained by invoking the time independence of the dipolar Hamiltonian $\tilde{H}_{\text{IS}}$ (eqn (23)). In contrast to the conventional CP and a number of its variants, it is the mixed frequencies Δ and Σ that determine the Hartmann–Hahn conditions.

2.1 Static case

Let us first consider the case of static samples, setting $\omega_r = 0$. Since ω_{1I} and ω_{2I} are positive, so is Σ. It follows that $\omega_{1S} = \Sigma > 0$ leads to a time-independent, zero-quantum component

$$\frac{1}{8}d_{\text{IS}}\sum_{k=-2}^{2} c_k(I_+S_- + I_-S_+), \qquad (26)$$

which is quite similar to the secular contribution found in the conventional CP schemes, except that the coefficient of the

flip-flop term, $d_{\text{IS}}/8$, is halved in the case of DONUT CP compared to that in the conventional CP, $d_{\text{IS}}/4$.

To obtain the Hartmann–Hahn conditions that involve Δ, we separately deal with the following three cases.

Case (i): $\omega_{1I} > \omega_{2I}$

Since $\Delta > 0$, we find that $\omega_{1S} = \Delta$ gives a time-independent term

$$-\frac{1}{8}d_{\text{IS}}\sum_{k=-2}^{2} c_k(I_+S_+ + I_-S_-), \qquad (27)$$

which carries the double-quantum flop-flop term. Thus, the polarization of the target spin S is expected to be enhanced negatively. The double-quantum exchange in stationary samples is one interesting feature of DONUT CP, in contrast to the conventional CP where it is possible only in rotating samples.[30]

Case (ii): $\omega_{1I} = \omega_{2I}$

$\Delta = 0$, and no $\omega_{1S} > 0$ interfering with the $e^{\pm i\Delta t}$ term is found.

Case (iii): $\omega_{1I} < \omega_{2I}$

$\Delta < 0$, and $\omega_{1S} = -\Delta > 0$ leads to the zero-quantum secular term, so that positive enhancement of the magnetization of the target spins S is expected.

The matching conditions and the corresponding secular terms responsible for polarization transfer are summarized in Table 1.

2.2 MAS case

In the case of MAS, the time dependence induced by the sample spinning can compensate for the energy mismatch. Thus, the Hartmann–Hahn conditions are found, irrespective of the mutual size relation between ω_{1I} and ω_{2I}. The zero-quantum secular term follows from

$$\omega_{1S} = -\Delta + n\omega_r, \qquad (28)$$

$$\omega_{1S} = \Sigma + n\omega_r, \qquad (29)$$

and the double-quantum term from

$$\omega_{1S} = \Delta + n\omega_r, \qquad (30)$$

$$\omega_{1S} = -\Sigma + n\omega_r, \qquad (31)$$

where $n = \pm 1, \pm 2$.

Now, the nutation frequency ω_{1S} for the target spins that fulfils the Hartmann–Hahn condition can be negative, as is also the case for the conventional CP.[30] The effect of negative ω_{1S} will be discussed below.

Table 1 The Hartmann–Hahn (H–H) conditions for stationary samples and the secular terms of the dipolar interaction under DONUT CP

	H–H condition	Secular terms
$\omega_{1I} > \omega_{2I}$	$\omega_{1S} = \Delta$	$\propto I_+S_+ + I_-S_-$
	$\omega_{1S} = \Sigma$	$\propto I_+S_- + I_-S_+$
$\omega_{1I} = \omega_{2I}$	$\omega_{1S} = \Sigma$	$\propto I_+S_- + I_-S_+$
$\omega_{1I} < \omega_{2I}$	$\omega_{1S} = -\Delta$	$\propto I_+S_- + I_-S_+$
	$\omega_{1S} = \Sigma$	$\propto I_+S_- + I_-S_+$

13840 | *Phys. Chem. Chem. Phys.*, 2023, **25**, 13838–13845

This journal is © the Owner Societies 2023

2.3 A note on the initial $\pi/2$ pulse

Let us recall the two conditions for CP to take place:[3] (a) the Hartmann–Hahn condition is fulfilled, (b) the magnetization of the source spins is locked along the effective field in the relevant frame of reference. So far, we have considered (a) alone. In the conventional CP, to fulfill (b), a $\pi/2$ pulse is applied to flip the magnetization of the source spin into the xy-plane before the pulse for the Hartmann–Hahn contact is applied, and the phase of the former has to be shifted by $\pi/2$ with respect to that of the latter. Interestingly, in DONUT CP, the initial $\pi/2$ pulse is unnecessary, provided that the z axis is chosen to be the axis of the second nutation, since, in the nutation frame, the only existing field points in the z direction, which is parallel to the initial magnetization of the source spin. It should be noted that, if the second nutation axis is not parallel to the z axis, the initial $\pi/2$ pulse is required.

3. Experimental

To let spins I evolve under $H_{rf}^I(t)$ given in eqn (2), the rf irradiation is applied with an amplitude $\omega_a(t)$ given by

$$\omega_a(t) = \sqrt{\omega_{1I}^2 + \omega_{2I}^2 \sin^2 \omega_{1I}t}, \tag{32}$$

with a phase $\phi(t)$

$$\phi(t) = \tan^{-1}\left[\frac{-\omega_{2I}\sin \omega_{1I}t}{\omega_{1I}}\right], \tag{33}$$

and a frequency offset $\Delta\omega(t)$

$$\Delta\omega(t) = \omega_{2I}\cos \omega_{1I}t. \tag{34}$$

To obtain the profile of such additional phase modulation that incorporates the frequency modulation (eqn (34)), we rewrite $H_{rf}^I(t)$ as

$$H_{rf}^I(t) = H_a^I(t) + H_b^I(t), \tag{35}$$

$$H_a^I(t) = \Delta\omega(t)I_z, \tag{36}$$

$$H_b^I(t) = \omega_a(t)[I_x\cos \phi(t) + I_y\sin \phi(t)]. \tag{37}$$

We also rewrite $U_I(t)$, originally given in eqn (1), as

$$U_I(t) = U_a(t)U_b(t), \tag{38}$$

where

$$U_a(t) = \exp\left[-i\int dt H_a^I(t)\right] = \exp\left[-i\frac{\omega_{2I}}{\omega_{1I}}\sin \omega_{1I}t I_z\right] \tag{39}$$

$$U_b(t) = T \exp\left[-i\int dt \tilde{H}_b^I(t)\right], \tag{40}$$

with

$$\begin{aligned}\tilde{H}_b^I(t) &= U_a^{-1}(t)H_b^I(t)U_a(t) \\ &= \omega_a(t)\{I_x\cos[\phi(t) - \psi(t)] + I_y\sin[\phi(t) - \psi(t)]\},\end{aligned} \tag{41}$$

$$\psi(t) = \frac{\omega_{2I}}{\omega_{1I}}\sin \omega_{1I}t. \tag{42}$$

In the interaction frame with respect to $H_a^I(t)$, the profile of the phase modulation is given by

$$\phi(t) - \psi(t), \tag{43}$$

while that of the amplitude modulation is unchanged and is given simply by $\omega_a(t)$. Examples of the waveforms of the amplitude $\omega_a(t)$ and the phase $\phi(t) - \psi(t)$ are given in the ESI.†

The relationship between the sign of the phase of the rf signal programmed by the user of an NMR spectrometer and the sign of the phase of the rf field that is actually produced has been discussed extensively. According to the instructive papers by Levitt,[10,11] when a pulse sequence involves phase modulation, it is necessary to set the sign of the phase depending on both the sign of the gyromagnetic ratio and the way that the carrier wave at the Larmor frequency ω_0 is generated in the transmitter of the spectrometer, through mixing of a pair of synthesized rf signals at an intermediate frequency ω_{IF} and a local frequency ω_{LO}. For spins with a positive gyromagnetic ratio, the sign of the phase needs to be reversed when the carrier signal is generated through up-conversion, namely $\omega_0 = \omega_{IF} + \omega_{LO}$, whereas the sign has to be kept unaltered in the case of down-conversion, $i.e.$, $\omega_0 = |\omega_{IF} + \omega_{LO}|$. It is recommended that the user of the spectrometer is aware of whether up-conversion or down-conversion is employed in the transmitter being used, so as to make the right choice of the sign of the phase.

In the present work, we implemented DONUT of the ^{1}H spins (positive gyromagnetic ratio) on home-built NMR spectrometers[31–33] in nominal 9.4 T and 7 T magnets, setting the intermediate frequency ω_{IF} at 180 MHz and the local frequency ω_{LO} at 220 MHz (120 MHz) + δ, mixing them in the transmitter to yield signals at $\omega_{IF} \pm \omega_{LO}$, and passing them through a 400 MHz (300 MHz) bandpass filter, thereby choosing $\omega_{IF} + \omega_{LO} = 400$ MHz (300 MHz) + δ. Here, δ, determined by the actual field strength, was on the order of several tens of kHz in this work. Thus, the signal was up-converted. Taking advantage of employing the open-architecture home-built spectrometer, we unambiguously chose to reverse the sign of the phase given in the pulse program.

To check if the sequence worked as intended, we carried out ^{1}H double-nutation experiments in liquid water. In Fig. 2, the first points of the quadrature-demodulated ^{1}H NMR signal, obtained after applying DONUT for incremented time intervals of up to 50 μs, are plotted. The data reflect the trajectory of the ^{1}H magnetization, initially in thermal equilibrium, onto the xy plane. The case of $(\omega_{1I}/2\pi, \omega_{2I}/2\pi) = (20$ kHz, 0 kHz), shown in Fig. 2(a), is simply the conventional nutation around the x axis, and the resultant trajectory is expected to draw a circular pattern on the yz plane, and its projection onto the xy plane showed a linear profile. For a finite $\omega_{2I}/2\pi$ of 10 kHz, the xy projection of the trajectory drew an arc (Fig. 2(b)). With increasing frequency $\omega_{2I}/2\pi$ of the second nutation, the deviation from the linear profile became more prominent (Fig. 2(c)–(f)).
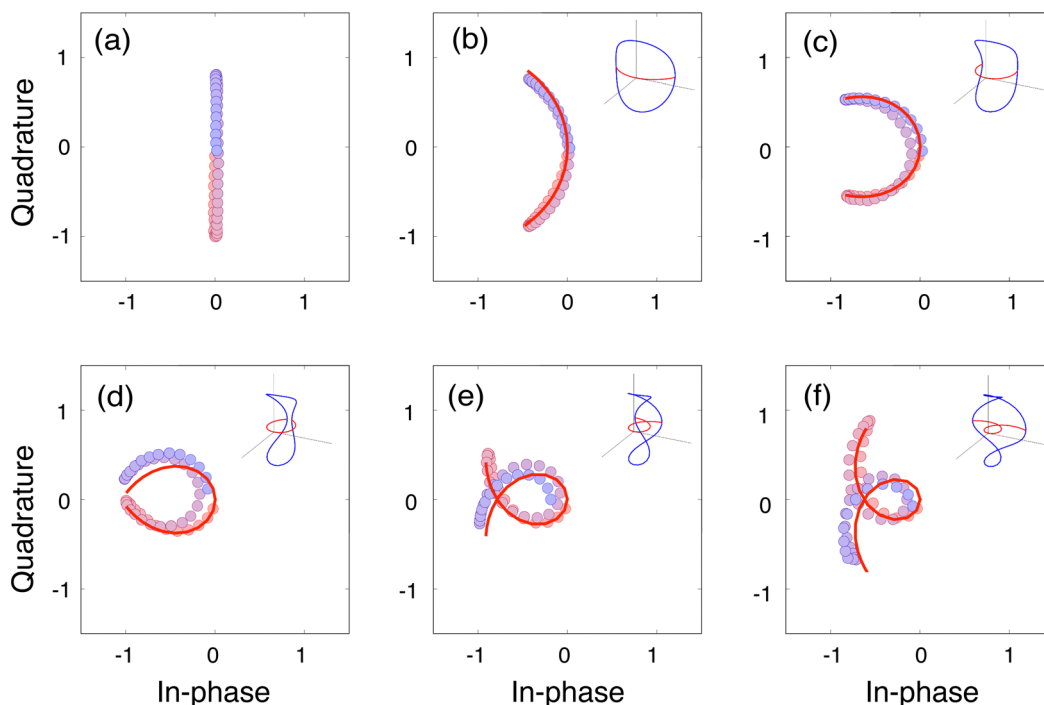
This journal is © the Owner Societies 2023

Phys. Chem. Chem. Phys., 2023, **25**, 13838–13845 | **13841**

Fig. 2 Trajectories of the ^{1}H magnetization of liquid water under double nutation applied with frequencies ($\omega_1/2\pi$, $\omega_2/2\pi$) of (a) (20 kHz, 0 kHz), (b) (20 kHz, 10 kHz), (c) (20 kHz, 20 kHz), (d) (20 kHz, 30 kHz), (e) (20 kHz, 40 kHz), and (f) (20 kHz, 50 kHz) for incremented time intervals up to 50 µs. The position of each circle represents the in-phase and the quadrature parts of the first sampling point of the measured FID. The magnitude of the complex data point was normalized to that obtained with the conventional $\pi/2$ pulse. Solid lines represent the trajectories of the magnetization (inset) and their projection onto the (x,y) plane obtained by numerically solving the Bloch equation with the initial magnetization being along the z axis and under application of the double-nutation by rf irradiation with amplitude $\omega_a(t)$ and phase $\phi(t) - \psi(t)$ given in eqn (32) and (43).

To examine the trajectory of the ^{1}H magnetization in the Bloch sphere, we numerically solved the Bloch equations,[34] under the rf irradiation corresponding to the Hamiltonian given in eqn (41), with a normalized initial magnetization to be (0,0,1). In Fig. 2(b)–(f), also shown are the calculated three-dimensional trajectories of the magnetization and its projection onto the xy plane, which were found to explain the observed dependence of the transverse magnetization on the duration of the DONUT pulse, and therefore convinced us that the pulse sequence of DONUT was indeed working as we intended.

4. Results and discussion

4.1 CP spectra

Fig. 3(a) shows ^{13}C magnetizations enhanced by DONUT CP obtained for a stationary powder sample of adamantane as a function of the amplitude ω_{1S} of the rf field applied to the target ^{13}C spins. Following Meier,[30] we henceforth refer to the ω_{1S} dependence of the S magnetization as the CP spectrum. The CP spectrum depicted with blue circles in the figure was obtained with DONUT applied to the source ^{1}H spins with nutation frequencies ($\omega_{1I}/2\pi$, $\omega_{2I}/2\pi$) of (20 kHz, 50 kHz), whereas the CP spectrum with the swapped combination, i.e., ($\omega_{1I}/2\pi$, $\omega_{2I}/2\pi$) = (50 kHz, 20 kHz), is shown with red circles. For both of these cases, time dependence with the
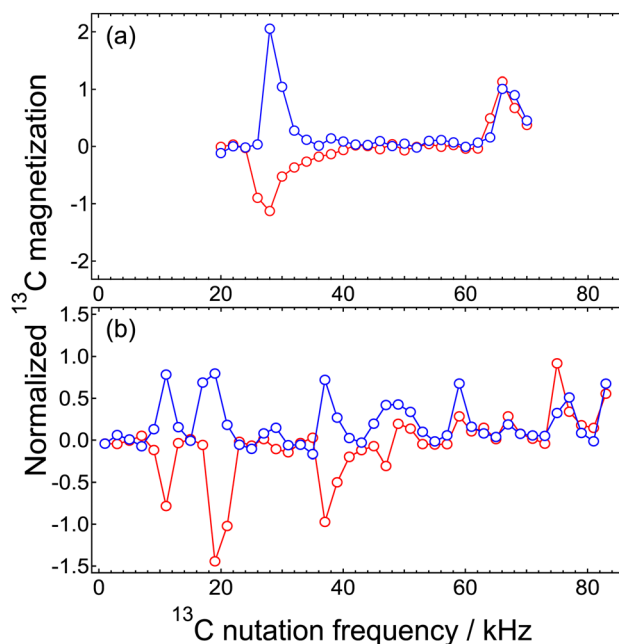

Fig. 3 ^{1}H–^{13}C Hartmann–Hahn matching profiles of DONUT CP measured for adamantane in a magnetic field of 7 T under (a) the static condition and (b) MAS at 9 kHz. Red and blue circles represent the ω_{1S} dependence obtained with ($\omega_{1I}/2\pi$, $\omega_{2I}/2\pi$) of (50 kHz, 20 kHz) and (20 kHz, 50 kHz), respectively. The contact time was 7 ms.

mixed frequencies $|\omega_{1I} \pm \omega_{2I}|$, namely, *ca.* $2\pi\cdot30$ kHz and $2\pi\cdot70$ kHz, is expected to develop. Indeed, when the ^{13}C nutation frequency ω_{1S} was closer to these values, the ^{13}C magnetization was enhanced, as demonstrated in Fig. 3(a). For $(\omega_{1I}/2\pi, \omega_{2I}/2\pi) = (50$ kHz, 20 kHz$)$, the ^{13}C magnetization was negatively enhanced for $\omega_{1S} \sim \Delta$ of around $2\pi\cdot30$ kHz. This is consistent with the theory discussed above, which derived the double-quantum nature of the secular component of the heteronuclear dipolar interaction in the nutation frame for the source spins and in the rotating frame for the target spins for the case of $\omega_{1I} > \omega_{2I}$.

In Fig. 3(b), the Hartmann–Hahn matching profiles, obtained with DONUT CP under MAS at 9 kHz, are shown. Now, the observed DONUT-CP spectrum was such that the individual peak in the static case (Fig. 3(a)) split into sidebands with a separation corresponding to the spinning speed, just like in the case of the conventional CP under MAS. The feature of negative enhancement for the case of $\omega_{1I} > \omega_{2I}$ and $\omega_{1S} = \Delta$ is retained.

Fig. 4 shows a ^{13}C DONUT-CP spectrum of the methylene carbon obtained in polycrystalline glycine under MAS at 23 kHz with DONUT applied at the ^{1}H spins with $(\omega_{1I}/2\pi, \omega_{2I}/2\pi)$ of $(90$ kHz, 60 kHz$)$. With $\omega_{1I} > \omega_{2I}$, $\Delta/2\pi = 30$ kHz, and $\omega_r/2\pi = 23$ kHz, the expected double-quantum exchange with negative enhancement of the ^{13}C magnetization was observed at around $\omega_{1S}/2\pi$ of 76 kHz ($n = 2$), 53 kHz ($n = 1$), and 7 kHz ($n = -1$). The positive peak of the DONUT-CP spectrum in Fig. 4 is assigned as the $n = -2$ sideband of the DONUT-CP spectrum, which ought to be at around $-2\pi\cdot16$ kHz, but folded back to the positive position at $|\Delta - 2\omega_r|$ of *ca.* $+2\pi\cdot16$ kHz. In addition, the zero-quantum exchange, instead of the double-quantum exchange, was observed for the folded-back peak. It is interesting to make a comparison with the well-known peak folding in the conventional CP under MAS, where the double-quantum exchange alone takes place for the folded-back peak.[30]
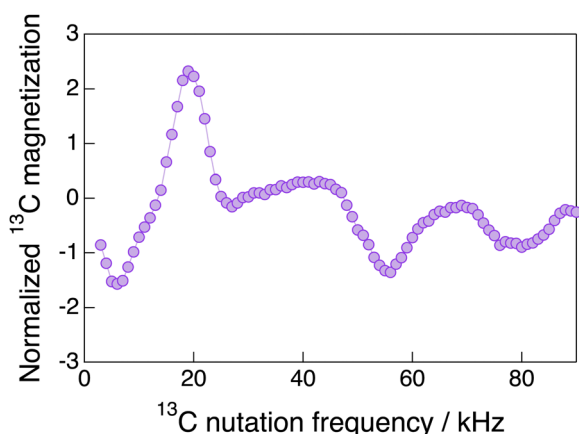

Fig. 4 ^{13}C nutation frequency dependence of methylene ^{13}C magnetization in 9.5%-2-^{13}C-labeled glycine under DONUT CP with $(\omega_{1I}/2\pi, \omega_{2I}/2\pi)$ of $(90$ kHz, 60 kHz$)$ in a magnetic field of 9.4 T under MAS at 23 kHz. The contact time was 0.15 ms.

4.2 Magnetization buildup

Fig. 5(a) shows a ^{15}N spectrum of a polycrystalline sample of ^{15}N-labeled histidine in the form of a τ tautomer (Fig. 5(b)).[35] The three peaks are assigned as the α, ε_2, and δ_1 sites, respectively, as indicated in the figure. Fig. 6 compares the buildup behaviors of the ^{15}N magnetizations in histidine under the conventional CP and the DONUT CP schemes under MAS at 20 kHz. In the former, the source ^{1}H spins were irradiated with continuous-wave (cw) rf with an intensity $\omega_{1I}/2\pi$ of 35 kHz, while in the latter, DONUT with $\omega_{1I}/2\pi = 80$ kHz and $\omega_{2I}/2\pi = 45$ kHz was applied. To the target ^{15}N spins, cw rf irradiation was applied with intensities of 17 kHz and 16 kHz, which were experimentally found to be optimal in the respective measurements.

For all three nitrogen sites in histidine, the initial buildup was slower in DONUT CP than in the conventional CP. Indeed, the slopes of the buildup curve at the beginning of the contact time were less steep by factors of 2.5, 2.1, and 2.0 for the α, ε_2, and δ_1 sites for DONUT CP compared to the conventional CP. For the ε_2 nitrogen, which has a covalent bond to the hydrogen atom and is therefore close to the latter, transient oscillation was observed. The period of oscillation in DONUT CP was found to be longer than that in the conventional CP by a factor of *ca.* 1.6. The slower buildup and the longer period of the transient oscillation are ascribed to the down-scaling of the heteronuclear dipolar interaction in the nutation frame by the factor of 2.

Interestingly, for the α and ε_2 sites, as the contact time was increased up to several hundreds of microseconds, the buildup curves for the conventional CP began to decay, while those for DONUT CP continued to grow. Eventually, for all three sites, DONUT CP led to larger ^{15}N magnetization when increasing the contact time further, up to several milliseconds. Since the way that the rf irradiation was applied to the ^{15}N spins was the same for both CP schemes, it was the relaxation of the ^{1}H spins that led to the difference.

When a spin species with a relatively low gyromagnetic ratio, like ^{15}N, is the target, it is often not feasible or desirable to apply too much rf power, such that one has to bear a relatively low nutation frequency ω_{1S}. Then, in the conventional CP, one has to reduce the intensity of the rf field applied to the source spins as well to fulfill the Hartmann–Hahn condition. Even
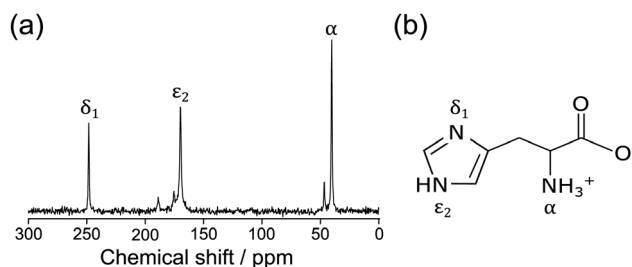

Fig. 5 (a) ^{15}N spectrum of polycrystalline ^{15}N-labeled histidine, obtained with DONUT CP in 9.4 T under MAS at 20 kHz with a contact time of 3 ms. (b) The structure of a neutral τ tautomer of histidine.
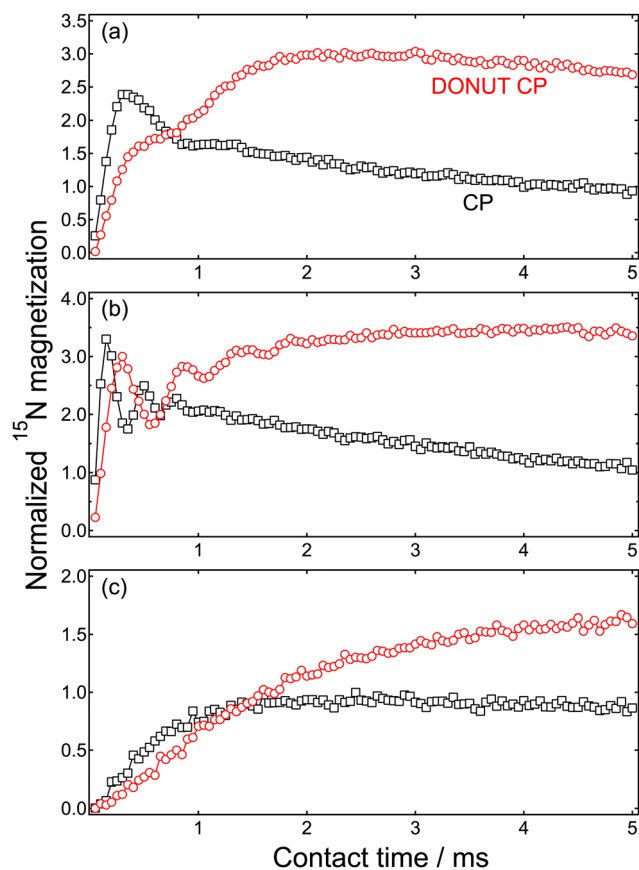
This journal is © the Owner Societies 2023

Phys. Chem. Chem. Phys., 2023, **25**, 13838–13845 | **13843**

Fig. 6 Contact-time dependence of the ^{15}N magnetization of (a) the α, (b) the ϵ_2 and (c) the δ_1 sites of ^{15}N-labeled polycrystalline histidine, measured in a magnetic field of 9.4 T under MAS at 20 kHz by DONUT CP (red circles) and conventional CP (black squares).

though this is not the case if one employs ultrafast MAS, access to such a state-of-art facility is still limited. In addition, ultra-fast MAS is not compatible with samples with a relatively large volume, which is often desirable to gain sensitivity. Even though the concept of time-averaged precession frequency (TAPF) can be a solution in CP to the low-gyromagnetic-ratio spin species, the ^{1}H relaxation can be so fast that it is difficult to optimize the performance of magnetization transfer.[36,37] Conversely, in DONUT CP, various combinations of ω_{1I} and ω_{2I} can be chosen such that the effect of relaxation is not so serious.

The overall profile of the CP buildup curve is determined by the balance between the two competing processes, namely transfer of polarization and relaxation. As discussed above, the polarization transfer was indeed slower in DONUT CP than in the conventional CP, because of the smaller magnitude of the secular heteronuclear dipolar interaction in the nutation frame. In DONUT CP, the arena in which spins I undergo relaxation is the nutation frame, in contrast to the rotating frame in the conventional CP schemes. Here, we introduce a symbol $T_{1\nu}$ to represent the time constant of spin–lattice relaxation of spins I in the nutation frame, in analogy with $T_{1\rho}$ that represents spin–lattice relaxation in the rotating frame.

The subscript ν (nu) appropriately reminds one of the nutation frame, just like the subscript ρ (rho) does of the rotating frame.

The dynamics of spin–lattice relaxation in the nutation frame require development of the method to experimentally determine $T_{1\nu}$, collection of data in a number of systems under various experimental conditions, and an extension of the relaxation theory that is well-established in the case of the rotating frame[3] by incorporating the relevant spin interactions. The expression for the effective homonuclear dipolar interaction under DONUT, already given in ref. 12 in the case of simultaneous nutations around the x and the y axes with a common rate $\omega_{1I} = \omega_{2I} = C$, includes quite a few terms, some of which can interfere with the time dependence caused by sample spinning. As a result, $T_{1\nu}$ as a function of ω_{1I}, ω_{2I}, and ω_r would show a somewhat complex profile. Although systematic studies on these subjects are outside the scope of the current work, what the results of DONUT CP demonstrated in this work imply is that, in some cases, spin–lattice relaxation in the nutation frame can be slower than that in the rotating frame. When this is indeed the case, the slower buildup rate due to the reduced heteronuclear dipolar interaction can be more than compensated for by the benefit of the longer $T_{1\nu}$.

5. Summary

The nutation frame is the interaction frame with respect to the Hamiltonian responsible for driving nutation. DONUT CP causes transfer of nuclear spin polarization in solids between the source spins in the nutation frame and the target spins in the rotating frame. The Hartmann–Hahn condition $\Delta = \omega_{1S}$ for $\omega_{1I} > \omega_{2I}$ leads to double-quantum exchange, and the other Hartmann–Hahn conditions to zero-quantum exchange. Under MAS, the peak of the DONUT-CP spectrum at the negative frequency folds back to the positive region, accompanying sign inversion in the intensity of the magnetization. In DONUT CP, the magnitude of the secular part of the dipolar interaction is half that in the conventional CP, resulting in a slower buildup rate. Nevertheless, there exist cases in which the maximum attainable enhancement exceeds that in the conventional CP, when spin relaxation in the nutation frame is slow enough.

Author contributions

Yu Wang: investigation, visualization, writing – original draft. Kazuyuki Takeda: conceptualization, supervision, investigation, visualization, writing – review & editing.

Conflicts of interest

There are no conflicts to declare.

Acknowledgements

13844 | *Phys. Chem. Chem. Phys.*, 2023, **25**, 13838–13845

This journal is © the Owner Societies 2023

Notes and references

1 A. Pines, M. Gibby and J. S. Waugh, *J. Chem. Phys.*, 1973, **59**, 569–590.

2 J. Schaefer and E. O. Stejskal, *J. Am. Chem. Soc.*, 1976, **98**, 1031–1032.

3 M. Mehring, *Principles of High Resolution NMR in Solids*, Springer-Verlag, Berlin, Heidelberg, New York, 2nd, edn, 1983.

4 S. Hartmann and E. Hahn, *Phys. Rev.*, 1962, **128**, 2042–2053.

5 A. Henstra, P. Ducksen, J. Schmidt and W. Wenckebach, *J. Magn. Reson.*, 1988, **77**, 389–393.

6 A. Henstra, P. Dirksen and W. Wenckebach, *Phys. Lett. A*, 1988, **134**, 134–136.

7 A. Henstra and W. Wenckebach, *Mol. Phys.*, 2008, **106**, 859–871.

8 A. Henstra and W. Wenckebach, *Mol. Phys.*, 2014, **112**, 1761–1772.

9 R. R. Ernst, G. Bodenhausen and A. Wokaun, *Principles of Nuclear Magnetic Resonance in One and Two Dimensions*, Oxford University Press, 1987.

10 M. H. Levitt, *J. Magn. Reson.*, 1997, **126**, 164–182.

11 M. H. Levitt and O. G. Johannessen, *J. Magn. Reson.*, 2000, **142**, 190–194.

12 N. Khaneja and N. C. Nielsen, *J. Chem. Phys.*, 2008, **128**, 015103.

13 L. A. Straasø, M. Bjerring, N. Khaneja and N. C. Nielsen, *J. Chem. Phys.*, 2009, **130**, 225103.

14 K. Takeda, A. Wakisaka and K. Takegoshi, *J. Chem. Phys.*, 2014, **141**, 224202.

15 Y. Ishii and T. Terao, *J. Chem. Phys.*, 1998, **109**, 1366.

16 A. C. Kolbert and A. Bielecki, *J. Magn. Reson., Ser. A*, 1995, **116**, 29–35.

17 R. Fu, P. Pelupessy and G. Bodenhausen, *Chem. Phys. Lett.*, 1997, **264**, 63–69.

18 S. Zhang, B. H. Meier, S. Appelt, M. Mehring and R. R. Ernst, *J. Magn. Reson., Ser. A*, 1993, **101**, 60–66.

19 S. Hediger, P. Signer, M. Tomaselli, R. R. Ernst and B. H. Meier, *J. Magn. Reson.*, 1997, **125**, 291–301.

20 S. Hediger, B. H. Meier and R. R. Ernst, *Chem. Phys. Lett.*, 1993, **213**, 627–635.

21 M. Baldus, D. Geurts, S. Hediger and B. Meier, *J. Magn. Reson., Ser. A*, 1996, **118**, 140–144.

22 S. Hediger, B. Meier and R. Ernst, *Chem. Phys. Lett.*, 1995, **240**, 449–456.

23 W. K. Peng and K. Takeda, *J. Magn. Reson.*, 2007, **188**, 267–274.

24 T. Matsunaga, I. Matsuda, T. Yamazaki and Y. Ishii, *J. Magn. Reson.*, 2021, **322**, 106857.

25 W. Peng, K. Takeda and M. Kitagawa, *Chem. Phys. Lett.*, 2006, **417**, 58–62.

26 K. Takeda, Y. Noda, K. Takegoshi, O. Lafon, J. Trébosc and J.-P. Amoureux, *J. Magn. Reson.*, 2012, **214**, 340–345.

27 S. Hediger, B. Meier, N. D. Kurur, G. Bodenhausen and R. Ernst, *Chem. Phys. Lett.*, 1994, **223**, 283–288.

28 G. Metz, X. Wu and S. O. Smith, *J. Magn. Reson., Ser. A*, 1994, **110**, 219–227.

29 S. Zhang, B. H. Meier and R. R. Ernst, *J. Magn. Reson., Ser. A*, 1994, **108**, 30–37.

30 B. Meier, *Chem. Phys. Lett.*, 1992, **188**, 201–207.

31 K. Takeda, *Rev. Sci. Instrum.*, 2007, **78**, 033103.

32 K. Takeda, *J. Magn. Reson.*, 2008, **192**, 218–229.

33 K. Takeda, *Annu. Rep. NMR Spectrosc.*, 2011, **74**, 355–393.

34 A. Abragam, *Principle of Nuclear Magnetism*, Oxford University Press, 1961.

35 S. Li and M. Hong, *J. Am. Chem. Soc.*, 2011, **133**, 1534–1544.

36 K. Takegoshi and C. McDowell, *J. Magn. Reson.*, 1986, **67**, 356–361.

37 Z. D. Žujović and G. A. Bowmaker, *J. Magn. Reson.*, 2006, **181**, 336–341.

This journal is © the Owner Societies 2023

Phys. Chem. Chem. Phys., 2023, **25**, 13838–13845 | **13845**